# Space-Charge Modulated Electrical Breakdown in Polyethylene Nanodielelctrics

**Article** *in* IEEE Nanotechnology Magazine · April 2018

DOI: 10.1109/MNANO.2018.2814088



**8 authors**, including:

Daomin Min
Xi'an Jiaotong University
**88** PUBLICATIONS **319** CITATIONS

SEE PROFILE

Weiwang Wang
Xi'an Jiaotong University
**34** PUBLICATIONS **153** CITATIONS

SEE PROFILE

Frechette, M. F.
Hydro-Québec
**355** PUBLICATIONS **1,818** CITATIONS

SEE PROFILE

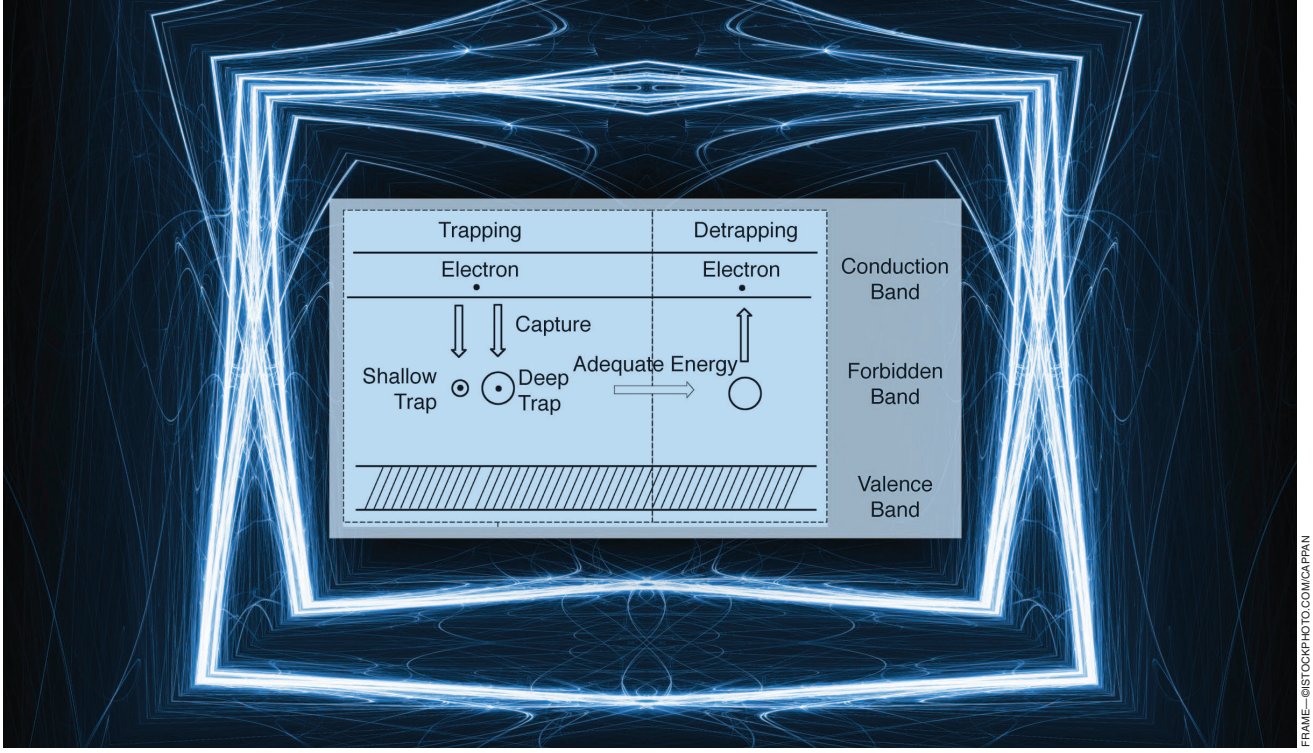


FRAME—©ISTOCKPHOTO.COM/CAPPAN

IN THIS ARTICLE, WE PROPOSE A method to calculate the density of deep traps formed in interaction zones based on a mesoscopic structure and a double-electric layer of polymer nanocomposites. A space-charge modulated breakdown model is then utilized to investigate the electrical breakdown property and its relation to deep traps in interaction zones. The deep traps that formed around the independent interaction zones suppressed the space-charge accumulation and the distortion of the electric field, leading to the improvement of the dc breakdown strength.

## INTERACTION ZONES IN NANOCOMPOSITES

Polymer nanocomposites have higher electrical breakdown strength than polymer matrices and their microcomposites, which is beneficial for the development of high-voltage dc power equipment [1]–[6].

# Space-Charge Modulated Electrical Breakdown in Polyethylene Nanodielectrics

## Its relation to deep traps in interaction zones.

DAOMIN MIN, CHENYU YAN, RUI MI, HAOZHE CUI, YUWEI LI, WEIWANG WANG, MICHEL FRÉCHETTE, AND SHENGTAO LI

*Digital Object Identifier 10.1109/MNANO.2018.2814088*
*Date of publication: 4 April 2018*

Intensive research has been conducted on nanocomposites, including thermal stability, mechanical property, and other electric properties [7]–[10]. It is widely accepted that the improvement of breakdown strength originates from the interaction zones or interfacial regions formed around nanoparticles. Interaction zones can change chain conformation, aggregation structure, or morphology of polymer matrices, causing the modifications of trap properties, carrier mobility, and charge injections, among others. These modifications lead to the suppression of space-charge accumulation, reduction of volume resistivity, and enhancement of electrical breakdown strength in polymer nanocomposites at low filler contents [3], [11]–[13].

The dispersion of nanoparticles and the mesoscopic structure of interaction zones largely determine the dielectric properties of polymer nanocomposites. The effect of interaction zones on electrical breakdown strength is not obvious at extremely low filler contents and is negligible, or even counterproductive, at high filler contents. In other words, the breakdown field increases and then decreases with an increase in filler content; it may also be saturated at high filler contents. Electrical breakdown strength (which relates positively to volume resistivity and space-charge accumulation [14]–[17]), volume resistivity, and space-charge accumulation all depend on filler content. The variation in charge transport properties produced by the interaction zones can change the accumulation of space charges, which may, in turn, modulate the electrical breakdown strength of polymer nanocomposites.

We introduce a model based on an interaction zone, from which shallow and deep-trap distributions can be obtained. Thus, the mechanics of a nanofiller's content impact on trap distribution and a trap distribution's impact on breakdown voltage will be analyzed.

## BREAKDOWN IN POLYETHYLENE NANOCOMPOSITES

Breakdown strength is the property that directly determines the long-term performance of nanocomposite dielectrics, which is influenced by many conditions, e.g., temperature, thickness, humidity, dispersion of the nanofiller. Kim showed that the dielectric strength of polytetrafluoroethylene was found to decrease with increasing temperatures for all sample thicknesses [18]. Additionally, the activation energy of dielectric strength increases with an increase in film thickness for the thinner film thickness range, but the activation energy is nearly constant for the thicker films, indicating that dielectric strength is less sensitive to fluctuations in temperatures for thicker films since the electromechanical breakdown is the dominant mechanism.

Min [19] proposed the charge transport and molecular displacement model to evaluate the space-charge accumulation and field distortion during the application of the dc ramp voltage on low-density polyethylene (LDPE) and found that the breakdown fiel d decreases exponentially with an increase in temperature. Zebouchi et al. [20] reported that the breakdown strength had a negative temperature dependence and a positive pressure dependence. (Frequency also had an impact on the breakdown strength.) The breakdown strength decreased with the increased frequency, and Artbauer [21] found that electric strength was also related to free volume and defects. He concluded that the breakdown is treated as the final stage of the disproportionate rise of the electron current in a very high field, and that the breakdown field depends on the same factors as the longest free path.

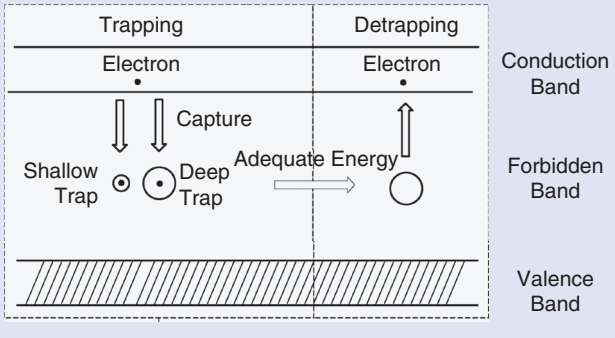


**FIGURE 1** The schematic of a charge capturing.

## TRAP THEORY

Random topological structures and chemical arrangements in polymers, also considered to be physical or chemical defects, can bring in many discontinuity points. An Anderson-localized state [22]–[24], which is also known as a *charge capture center* (trap), will capture free-moving charges. Traps in polymer materials can offer contributions to charge mobility and charge capture. Specifically, carriers (charges) directionally migrate under the effect of the electric field and contribute to conduction current; once these carriers are captured by traps, carrier density will decrease.

Trap density distribution in polymeric material can turn on various situations since traps that are constrained at a certain energy depth may exist in the material. Mizutani et al. [25] investigated the phenomenon of a transient space charge that restricts current and obtained the carrier mobility of a sample that varies from 50 to 90 °C. Their work demonstrated that carrier mobility of the high-density polyethylene sample obeys the Arrhenius equation and the trap energy is approximately 1.2 eV. Additionally, Dennison et al. [26] investigated the voltage–current response of the LDPE sample and simulated the results using a thermal-hopping conductivity model. The trap energy of the sample that was obtained was roughly 0.76 eV.

It is also possible for traps to be constrained in more than one energy level; Chen et al. [27], [28] proposed a space-charge accumulation and a decay model, based on double-discrete, energy-level traps. They measured the space-charge accumulation and decay properties of LDPE via a pulsed electro-acoustic measurement with voltage applied for 2 min and 10 min, respectively. As a result, they found that the energies of double traps are 0.88 eV and 1.01 eV, respectively.

Additionally, a trap may also exponentially distribute the trap energy level, as shown in Figure 1. Quirke et al. [29], [30] investigated the physical and chemical

defects in the distribution properties of PE via a molecular simulation method and concluded that trap distribution complies with exponential distribution, where the coefficient of the exponential function $N_{t0}$ is roughly $10^{26} - 10^{27}$ $m^{-3}$. Furthermore, traps may obey a Gauss distribution with trap energy. Simmons's theory can be applied to the isothermal decay current [31], the surface potential decay [32]–[35], or the thermally stimulated current method [36], and serve to obtain the trap density and distribution properties of materials. For polymeric materials, all of the results revealed that trap distribution can be regarded as a Gauss distribution or a combination of several Gauss distribution situations.

Carrier capturing is a significant process that influences the electric property of polymeric materials. If no trap exists in a dielectric, all of the charges can move freely with no barriers. Carrier mobility is then solely determined by charges, phonons, and the impurities' collision properties. Defects are inevitable in materials, and the effect of the traps' capturing charges must be noted, as shown in Figure 1, [22], [37]. Accompanied by a charge motion, some charges leave the conduction band and drop into the forbidden band. Traps in the forbidden band then capture the charges and are forced to be constrained in the forbidden band for a specific duration, which is determined by trap energy. Higher trap energy will lead to a longer retention time, which can increase exponentially with trap energy until the trapped-in charges obtain adequate energy to detrap and continue to move; thus, a trap-capturing effect can decrease the affected carrier's mobility, which is also called *effective carrier mobility*.

Generally, various retention times can vary by more than ten orders of magnitude, e.g., the retention time of a trap with an energy level of 0.1 eV is approximately $10^{-13}$ s, whereas it is roughly 500 s when the trap energy is 1 eV [38]. In most models, including ion- or electron-hopping conduction, trap-constrained conduction and Pool-Frankel conduction, the effective carrier mobility will decrease exponentially with an increase to the trap depth [22], [37], [38].

When explaining the breakdown property via the trap theory, four elements are taken into consideration: electrons and holes injection, the carrier mobilities of electrons and holes controlled by shallow traps, the trapping-in and trapping-out process of charges in deep traps and electron-hole combination (including free-electron free-hole recombinations), and the free-electron hole-trap recommendation and trap-electron free-hole recommendation. These elements are displayed in Figure 2.

## ESTIMATION OF DEEP-TRAP DENSITY IN NANODIELECTRICS

We propose the following model to calculate the density of deep traps formed by interaction zones for polymer nanocomposites: a space-charge modulated electrical breakdown model consisting of a bipolar charge injection and transport (i.e., the variation in trap density caused by interaction zones) and a breakdown criterion are used to investigate the affected mechanisms of filler content on the dc electrical breakdown field.

Several models, such as Lewis's model [39], [40], Tanaka's multicore model [5], [41], and Li's multiregion structure model [24] have been proposed to describe the interaction zones formed in polymer nanocomposites. Figure 3 shows the mesoscopic structures and charge distribution in interaction zones. From the mesoscopic structural point of view, interaction zones can be divided into three layers, i.e., the bonded, transitional, and normal regions [5], [41]. The thickness is several nanometers for the bonded region, approximately 10 nm for the transitional region, and greater than 10 nm for the normal region [5], [41], [42]. A

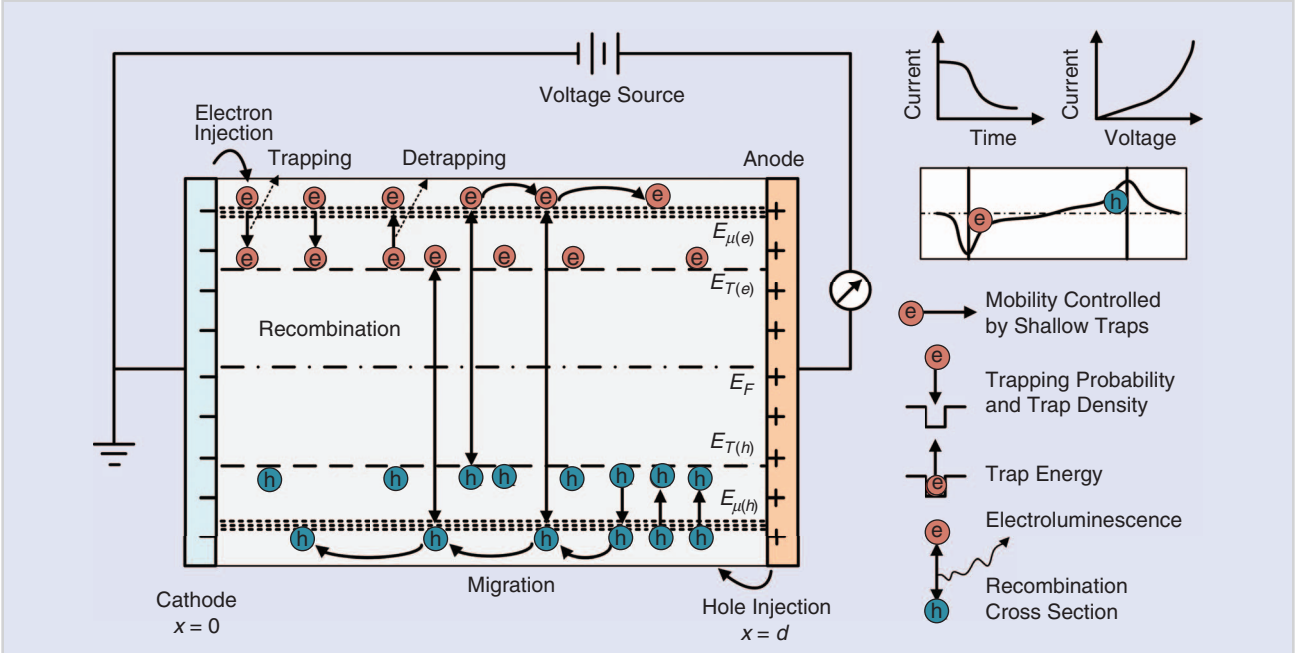


**FIGURE 2** A charge transport property during the breakdown process.

Gouy–Chapman diffuse layer or an electric double layer is formed in the interaction zone from the electrical point of view. The Gouy–Chapman diffuse layer overlaps the bonded, transitional, and normal regions [5], [41], [42]. The mesoscopic structure and the Gouy–Chapman layer in interaction zones modify charge transport properties, e.g., trap density and energy, the charge-trapping coefficient, carrier mobility, and the charge-injection barrier; consequently, the macroscopic properties are changed. In our experiments, we concentrated on the influence of the modification of trap density on the electrical breakdown of polymer nanocomposites.

The density of deep traps may be determined by the interparticle distance, thickness of the bonded and transitional regions, binding strength in the bonded layer, and overlapping of the Gouy–Chapman diffuse layers as shown in Figure 3 [5], [42]. The spherical inorganic nanoparticles with a density of $p_p$ and a weight of $m_n$ are incorporated into a semicrystalline polymer matrix with a density of $p_p$ and a weight of $m_p$ to prepare a polymer nanocomposite. The radius of nanoparticles is $r_n$, and they are assumed to be homogeneously dispersed in the polymer matrix with interparticle distance from surface-to-surface of $l_n$ and, therefore, mainly located in the amorphous regions [43]. The crystallinity is assumed to be $\chi_c$ for polymer nanocomposites. The weight fraction of nanofillers $f_m$ is equal to $m_n/(m_n+m_p)$, while the volume fraction $f_v$ is $m_n\rho_p/(m_n\rho_p+m_p\rho_n)$. Then, the relation between volume fraction $f_v$ and weight fraction $f_m$ can be obtained from the following equation

$$\frac{1}{f_v}=\frac{1}{f_m}\frac{\rho_n}{\rho_p}\left[1-f_m\left(1-\frac{\rho_p}{\rho_n}\right)\right]. \quad (1)$$

The volume fraction of nanoparticles $f_v$ can be expressed by

$$f_v=(1-\chi_c)\frac{4\pi}{3}\left(\frac{r_n}{2r_n+l_n}\right)^3. \quad (2)$$

The interparticle distance can be calculated from (2) and (1). Then, we can obtain the relation between the interparticle distance, weight fraction, densities of nanoparticles and the polymer matrix, and diameter of nanoparticles [5], [41], [44] as

$$l_n=\left[\left[\frac{4\pi(1-\chi_c)}{3}\frac{1}{f_m}\frac{\rho_n}{\rho_p}\left[1-f_m\left(1-\frac{\rho_p}{\rho_n}\right)\right]\right]^{\frac{1}{3}}-2\right]r_n. \quad (3)$$

The number density of nanoparticles $n_n$ is inversely proportional to the cubic volume with a length of $(l_n+l_{ip})$. The interspacing between the centers of two nanoparticles is $2r_n+l_n$. If we assume nanoparticles are distributed uniformly in the polymer matrix, the relation between the number density of nanoparticles and interspacing can be described by

$$n_n=(1-\chi_c)/(2r_n+l_n)^3. \quad (4)$$

Since the morphology of polymers becomes less ordered from the bonded layer to the loose layer, the energy of the traps decreases as the distance from the nanoparticle surface increases. Deep traps are formed in the bonded and transitional regions, whereas shallow traps are present in the normal region [5], [41]. Consequently, the density of deep traps is influenced only by the volume fraction of the bonded and transitional regions. The average distance between two deep traps in bonded and transitional regions is assumed to be $\lambda_{DT}$, and the number of deep traps $\zeta$ generated in an interaction zone can be calculated by the following equation:

$$\xi=\frac{4\pi}{3}\frac{r_{br}^3-r_n^3}{\lambda_{DT}^3}, \quad (5)$$

where $r_{br}$ is the radius of the transitional region. When the interfacial thickness is very small, it is extremely difficult to form deep traps. In other words, the density of deep traps in interfacial regions would be zero. With the increase in $l_{in}$, more deep traps will be generated in interfacial regions.

It is possible for the Gouy–Chapman layers to overlap with each other at high filler contents. The overlapping probability may increase dramatically with an increase in filler content. Accordingly, the possibility for independent interaction zones decreases strikingly.

$$P_i=\left[1+\left(\frac{32}{3}\pi n_n\frac{r_{gc}^6}{r_n^3}\right)^\beta\right]\exp\left[-\left(\frac{32}{3}\pi n_n\frac{r_{gc}^6}{r_n^3}\right)^\beta\right], \quad (6)$$

where $r_{gc}$ is the radius of the Gouy–Chapman layer, while $\beta$ is an exponent for the stretched exponential function.

The density of deep traps in interfacial regions also depends on the type of nanoparticles, the surface treatment,

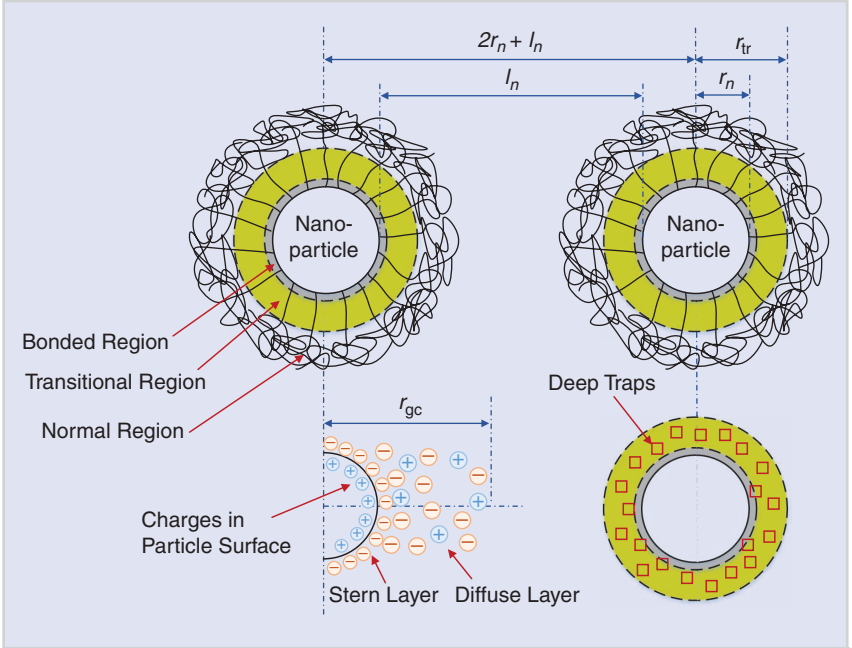


**FIGURE 3** A schematic of mesoscopic structures and charge distribution in an interaction zone. Deep traps are mainly formed in bonded and transitional regions.

charge distribution in the Gouy–Chapman diffuse layer, the binding strength in the first layer, and so on. Therefore, the density of deep traps can be written as

$$N_{DT} = \xi n_n P_t. \quad (7)$$

Figure 4 demonstrates how the density of deep traps formed in interaction zones changes with filler content in LDPE-based alumina ($Al_2O_3$) nanocomposites with a crystallinity of roughly 50%. The densities of the polymer matrix and the nanofillers were 0.918 and 4.0 gcm$^{-3}$, respectively. The radii of nanoparticles, the transitional region, and the Gouy–Chapman layer were 15, 30, and 125 nm, respectively. The average distance between the two deep traps in the bonded and transitional regions was assumed to be 3 nm. Independent interaction zones increase with a rise in filler content at relatively low values, which resulted in an increase to the deep traps. At relatively high filler contents, the Gouy–Chapman layers overlapped with each other, causing a decrease in independent interaction zones, and therefore deep traps.

A space-charge modulated electrical breakdown model [19] was utilized to simulate the breakdown strength of LDPE/$Al_2O_3$ nanocomposites at various filler contents. The electrons and holes were injected into the material from the cathode and the anode, respectively, by Schottky thermionic emission [45], [46]. Charge injection and transport in an insulating material were governed by a set of self-consistent equations, including equations of charge injection, charge continuity, transport, and Poisson's equation [19], [45], and [47]–[49], as follows:

$$j_{in(e,h)}(t) = AT^2 \exp\left(-\frac{E_{in(e,h)}}{k_B T}\right) \exp\left(\frac{\sqrt{eF/4\pi\varepsilon_0\varepsilon_r}}{k_B T}\right), \quad (8)$$

$$\frac{\partial q_{free}(x,t)}{\partial t} + \frac{\partial q_{trap}(x,t)}{\partial t} + \frac{\partial j_c(x,t)}{\partial x} = 0, \quad (9)$$

$$j_c(x,t) = q_{free}(x,t)\mu_0 F(x,t), \quad (10)$$

$$\frac{\partial^2 \phi(x,t)}{\partial x^2} = -\frac{q_{free}(x,t) + q_{trap}(x,t)}{\varepsilon_0 \varepsilon_r}. \quad (11)$$

Here, $A$ is the Richardson constant ($= 1.20 \times 10^6$ $a.m.^{-2}K^{-2}$), and $k_B$ is the Boltzmann constant. Furthermore, $t$ is the time after applying voltage in seconds, while $F(0,t)$ and $F(0,t)$ are the electric fields at the interfaces $x = 0$ and $x = d$, respectively. The injection currents from the cathode and the anode, $j_{in(e)}$ and $j_{in(h)}$, respectively, are determined by contact with the potential barrier between the material and its electrodes, $E_{in(e)}$ and $E_{in(h)}$, the electric fields at interfaces, and temperature.

LDPE/$Al_2O_3$ nanocomposites with various filler contents ranging from 0 wt% to 10 wt% were used for dc breakdown simulations. The nanocomposite films were 200 $\mu$m in thickness, and in the dc breakdown simulations, LDPE/$Al_2O_3$ nanocomposite films were discretized into 500 elements, and each element was 0.4 $\mu$m in length. The computation time step $\Delta t$ was 1 ms, and the nonlinear charge continuity shown in (9) was numerically solved by a finite differential weighted essentially nonoscillatory method, which consists of fifth-order spatial discretization and explicit third-order total variation diminishing Runge–Kutta time discretization. As expressed in (11), The Poisson's was solved by a boundary element method.

Deep traps in polymer nanocomposites consist of those in interfacial regions with a density of $N_{Tn}$, and in the polymer matrix with a density of $N_{Tp}$. It can be assumed that deep traps in interfacial regions and those in the polymer matrix are located in the same energy level. Consequently, the density of deep traps in polymer nanocomposites $N_T$ is equal to the summation of $N_{Tn}$ and $N_{Tp}$, i.e., $N_T = N_{Tn} + N_{Tp}$.

A ramp voltage with a rising rate of 500 Vs$^{-1}$ was applied on the nanocomposite films. An intrinsic breakdown strength was set for LDPE nanocomposites, meaning that dc breakdown simulations stop when the internal local electric field reaches 365 kV/mm. The breakdown field was then calculated from the applied voltage, divided by the sample thickness.

Figure 5 displays the comparison between simulated and experimental results of the dc breakdown field as a function of filler content in a range of 0 wt% to 10 wt% in LDPE/$Al_2O_3$ nanocomposites. The simulation results are in good

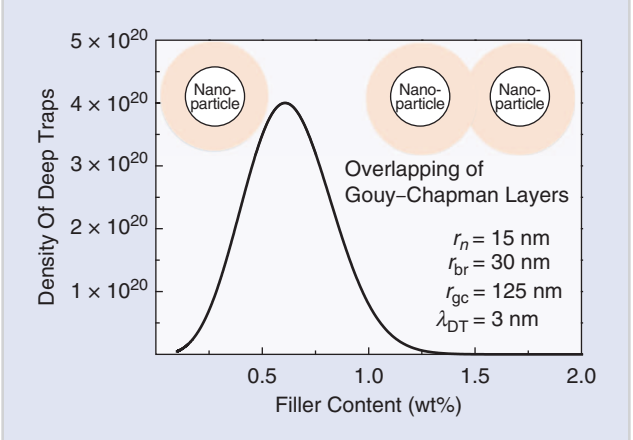


**FIGURE 4** The density of deep traps formed in interaction zones as a function of filler content in LDPE/$Al_2O_3$ nanocomposites.

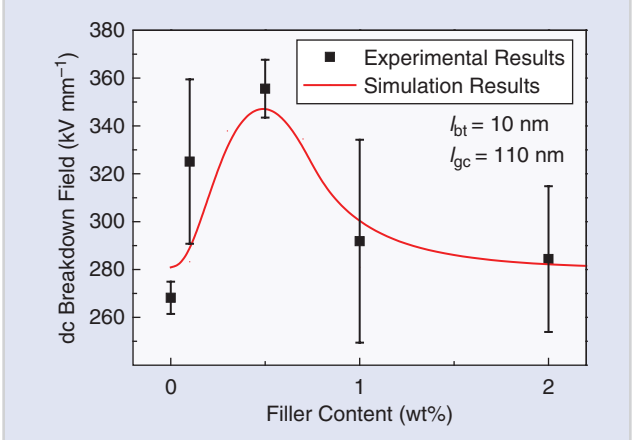


**FIGURE 5** The dc breakdown field as a function of filler content of polymer nanocomposites.

Breakdown strength is the property that directly determines the long-term performance of nanocomposite dielectrics, which is influenced by many conditions, e.g., temperature, thickness, humidity, dispersion of the nanofiller.

agreement with experiments. The dc breakdown field obtained by simulation first increases and then decreases with an increase in filler content. The breakdown field reaches its maximum at a filler content of approximately 0.5 wt% and becomes saturated above 2 wt%.

Figures 6 and 7 show the distributions of space charges and electric fields at various times during the voltage rise stage. Electrons and holes are injected into dielectric materials under an applied voltage through Schottky thermionic emission from the electrode and the anode, respectively. These injected negative and positive charges migrate in the bulk of materials toward the opposite electrodes via extended states and/or shallow traps. During the migration, these charges may be captured by deep traps produced by chemical impurities and interfacial regions between nanoparticles and the polymer matrix. Homocharges are then accumulated near the electrodes, while the electric field in the bulk of the materials is distorted by the accumulated space charges. The electric field is enhanced in the middle of the materials while it is reduced near the electrodes. The maximum electric field increases with time and reaches the intrinsic breakdown strength at s. The breakdown electric field is determined to be kV/mm from the applied voltage. The same simulation is carried out for LDPE

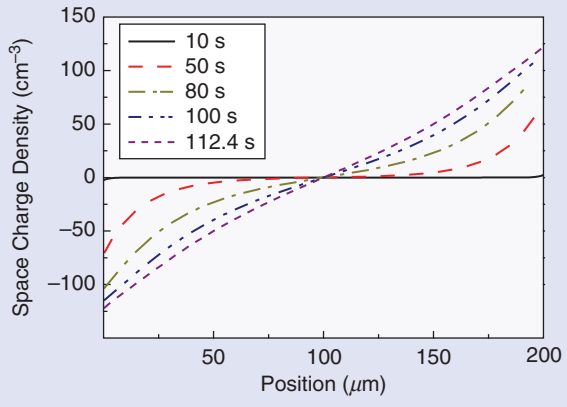


**FIGURE 6** The space charge distributions in neat LDPE at various times during the voltage rise stage.

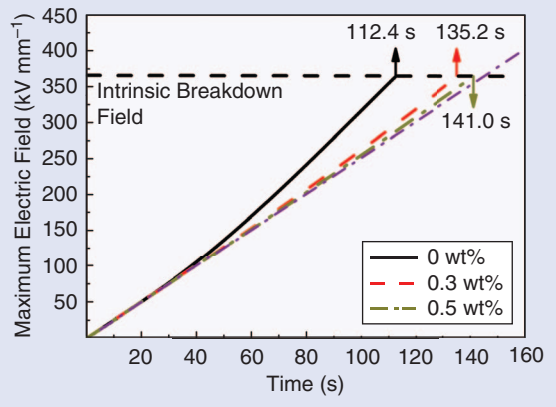


**FIGURE 8** The average space charge density as a function of filler content in LDPE nanocomposites after applying a ramping voltage for 110 s.

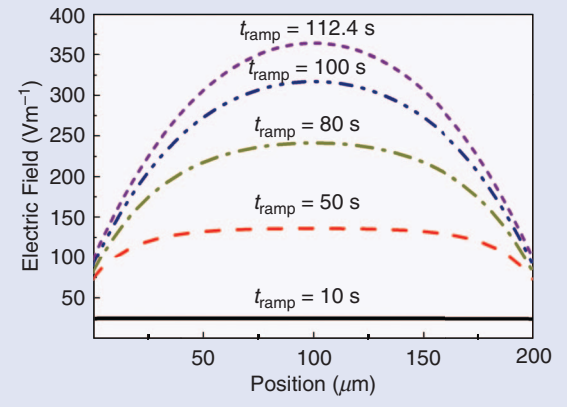


**FIGURE 7** The electric field distributions in neat LDPE at various times during the voltage rise stage.

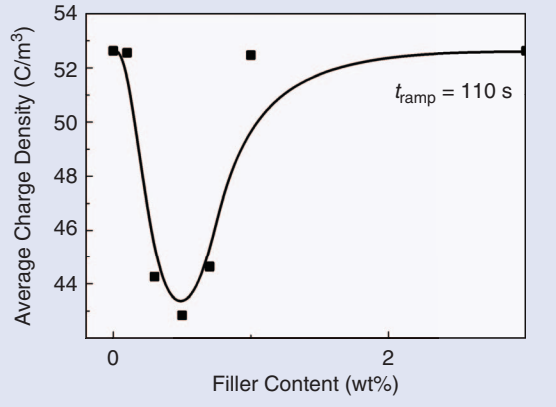


**FIGURE 9** The average space charge density as a function of filler content in LDPE nanocomposites after applying a ramping voltage for 110 s.

nanocomposites with different filler contents of nano-$Al_2O_3$.

The changes in the dc breakdown field with an increase in filler content can be observed by the variation in the space-charge accumulation and the electric field distortion in the polymer nanocomposites. Figures 3 and 6–9 reveal how the distributions of space charges and electric fields vary with increased filler content.

The thickness of the Gouy–Chapman diffuse layer determines the chance of overlap with a given filler content; this probability of overlap decreases with a decrease in the thickness of the Gouy–Chapman diffuse layer. The maximum dc breakdown field may occur at higher filler content, and this is observed in LDPE-based magnesium-oxide nanocomposites. The thickness of the Gouy–Chapman diffuse layer is determined by the charge density absorbed on the surface of nanoparticles. As shown in Figure 10, an increase in the thickness of the Gouy–Chapman diffuse layer, the transition point moved left to the lower nanofiller content. Additionally, for a specific Gouy–Chapman diffuse layer, the dc breakdown rose with an increase of field thicknesses of bonded and transitional regions, as seen in Figure 11.

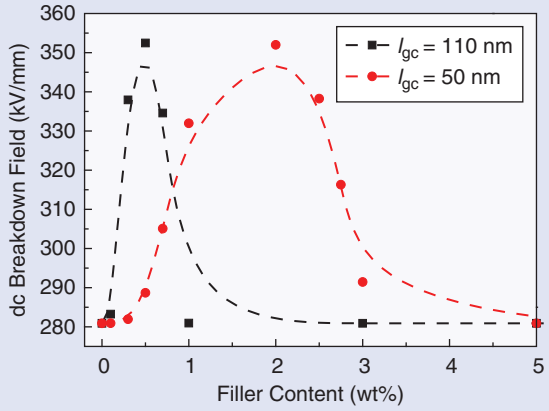


**FIGURE 10** The dc breakdown field as a function of filler content at different thicknesses of the Gouy–Chapman diffuse layer.

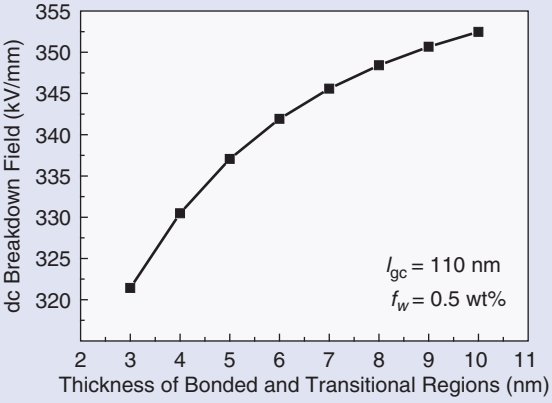


**FIGURE 11** The dependence of the dc breakdown field on the thickness of bonded and transitional regions at $l_{gc}$ and $f_w$ of 110 nm and 0.5 wt%.

## EVALUATION OF THE MODEL

This model explained the macroscopic electric phenomenon in terms of microscopic perspectives, and systematically analyzed the combination of nanofiller content with the dc breakdown field. The mechanism of how trap distribution and density affect properties of material, which can be considered as a valid method in nanocomposite research, were also demonstrated by this model. However, further efforts must be taken to explain the aggregative state of nanoparticles so that the effect of interfaces and their coordinated impact on electric strength, and the regulation and mechanics of breakdown behavior can be clearly understood.

## CONCLUSION

The density of deep traps formed in polymer nanocomposites was calculated by observing the mesoscopic structures and double electric layer around the interaction zones. The estimation method of deep-trap density was used in a space-charge modulated breakdown model to calculate the breakdown strength of polymer nanocomposites. The relation between the breakdown strength and the filler content was obtained and the simulation results were in good agreement with experiments. Deep traps formed around independent interaction zones at relatively low-filler content were found to suppress the accumulation of space charges and the distortion of the electric field, leading to the improvement of the breakdown strength. The proposed model is advantageous for exploring the influential mechanisms of the interaction zone on the electrical property of polymer nanocomposites.


## ACKNOWLEDGMENTS

This work was supported by the National Basic Research Program of China (Project 2015CB251003) and National Natural Science Foundation of China (Projects 51507124 and 51337008). It was also supported by State Key Laboratory of Power System of Tsinghua University (SKLD16KZ04).


## ABOUT THE AUTHORS


***Daomin Min*** (forrestmin@foxmail.com) is with the State Key Laboratory of Electrical Insulation and Power Equipment, Xi'an Jiaotong University, China.

***Chenyu Yan*** (leo-chenyu.yan@stu.xjtu.edu.cn) is a graduate student studying charge transport characteristics and analysis at Xi'an Jiaotong University, China.

***Rui Mi*** (mr2017@stu.xjtu.edu.cn) is a graduate student studying the breakdown characteristics of LDPE nanocomposites at Xi'an Jiaotong University, China.

***Haozhe Cui*** (cuihz0703@mail.xjtu.edu.cn) is a graduate student studying the breakdown characteristics of epoxy resin nanocomposites at Xi'an Jiaotong University, China.

***Yuwei Li*** (mirana111@stu.xjtu.edu.cn) is a graduate student studying energy storage properties of polymide nanocomposites at Xi'an Jiaotong University, China.

***Weiwang Wang*** (weiwwang@xjtu.edu.cn) is with the State Key Laboratory of Electrical Insulation and Power Equipment, Xi'an Jiaotong University, China.

***Michel Fréchette*** (frechette.mick@gmail.com) is with the State Key Laboratory of Electrical Insulation and Power Equipment at Xi'an Jiaotong University, China.

***Shengtao Li*** (sli@mail.xjtu.edu.cn) is with the State Key Laboratory of Electrical Insulation and Power Equipment at Xi'an Jiaotong University, China.

## REFERENCES

[1] P. Barber, S. Balasubramanian, Y. Anguchamy, S. Gong, A. Wibowo, H. Gao, H. Ploehn, and H. zur Loye, "Polymer composite and nanocomposite dielectric materials for pulse power energy storage," *Materials*, vol. 2, no. 4, pp. 1697–1733, 2009.

[2] D. Galpaya, "Synthesis, characterization and applications of graphene oxide-polymer nanocomposites," *Nature*, vol. 448, no. 7152, pp. 457, 2015.

[3] M. Roy, J. K. Nelson, R. K. Maccrone, L. S. Schadler, C. W. Reed, and R. Keefe, "Polymer nanocomposite dielectrics-the role of the interface," *IEEE Trans. Dielectr. Electr. Insul.*, vol. 12, no. 4, pp. 629–643, 2005.

[4] S. Singha and M. J. Thomas, "Dielectric properties of epoxy nanocomposites," *IEEE Trans. Dielectr. Electr. Insul.*, vol. 15, no. 1, pp. 12–23, 2008.

[5] T. Tanaka, "Dielectric nanocomposites with insulating properties," *IEEE Trans. Dielectr. Electr. Insul.*, vol. 12, no. 5, pp. 914–928, 2005.

[6] C. A. Wilkie and A. B. Morgan, "Polymer nanocomposites," *J. Polym. Sci. Part B, Polym. Phys.*, vol. 45, no. 24, pp. 3252–3256, 2010.

[7] A. Leszczyńska, J. Njuguna, K. Pielichowski, and J. R. Banerjee, "Polymer/montmorillonite nanocomposites with improved thermal properties: Part I. Factors influencing thermal stability and mechanisms of thermal stability improvement," *Thermochimica Acta*, vol. 453, no. 2, pp. 75–96, 2007.

[8] J. Castellon, H. Yahyaoui, O. Guille, E. David, M. Guo, and M. F. Fréchette, "Dielectric properties of POSS/LDPE and MgO/LDPE nanocomposites compounded by different techniques," in *Proc. IEEE Conf. Electrical Insulation and Dielectric Phenomena*, 2017, pp. 457–460.

[9] S. B. Ghafarizadeh, M. F. Fréchette, and E. David, "Fabrication and dielectric, mechanical, and thermal properties of low-density polyethylene (LDPE) composites containing surface-passivated silicon ($Si/SiO_2$ core/shell nanoparticles)," *Polym.-Plastics Technol. Eng.*, vol. 57, no. 4, pp. 327–334, June 2017. doi: 10.1080/03602559.2017.1326138.

[10] S. C. Tjong, "Structural and mechanical properties of polymer nanocomposites," *Mater. Sci. Eng.: R: Rep.*, vol. 53, no. 3, pp. 73–197, 2006.

[11] Y. Shen, Y. H. Lin, and C. W. Nan, "Interfacial effect on dielectric properties of polymer nanocomposites filled with core/shell-structured particles," *Adv. Functional Mater.*, vol. 17, no. 14, pp. 2405–2410, 2007.

[12] P. Rittigstein and J. M. Torkelson, "Polymer-nanoparticle interfacial interactions in polymer nanocomposites: confinement effects on glass transition temperature and suppression of physical aging," *J. Polym. Sci. Part B, Polym. Phys.*, vol. 44, no. 20, pp. 2935–2943, 2006.

[13] H. Shi, A. T. Lan, and T. J. Pinnavaia, "Interfacial effects on the reinforcement properties of polymer–organoclay nanocomposites," *Chem. Mater.*, vol. 8, no. 8, 1996.

[14] Y. Murakami, M. Nemoto, S. Okuzumi, S. Masuda, M. Nagao, N. Hozumi, Y. Sekiguchi, and Y. Murata, "DC conduction and electrical breakdown of MgO/LDPE nanocomposite," *IEEE Trans. Dielectr. Electr. Insul.*, vol. 15, no. 1, pp. 33–39, 2008.

[15] T. Okazaki, S. Okuzumi, S. Imazawa, Y. Murakami, M. Nagao, Y. Sekiguchi, C. Reddy, and Y. Murata, "Electric characteristics of MgO/LDPE nanocomposite up to breakdown under dc ramp voltage," in *Proc. Con. Electrical Insulation and Dielectric Phenomena*, Virginia Beach, 2009, pp. 654–657.

[16] Y. Murakami, et al. "Space charge measurement in MgO/LDPE nanocomposite up to breakdown under dc ramp voltage," *IEEE Trans. Elect. Electron. Eng.*, vol. 5, no. 4, pp. 395–399, 2010.

[17] Y. Murakami, S. Okuzumi, M. Nagao, and M. Fukuma, "The space charge measurement in MgO/LDPE nanocomposite up to the breakdown under dc ramp voltage," in *Proc. Int. Symp. Electrical Insulating Materials (ISEIM)*, 2008, pp. 159–162.

[18] H. K. Kim and F. G. Shi, "Thickness dependent dielectric strength of a low-permittivity dielectric film," *IEEE Trans. Dielectr. Electr. Insul.*, vol. 8, no. 2, pp. 248–252, 2001.

[19] D. Min, S. Li, and Y. Ohki, "Numerical simulation on molecular displacement and dc breakdown of LDPE," *IEEE Trans. Dielectr. Electr. Insul.*, vol. 23, no. 1, pp. 507–516, 2016.

[20] N. Zebouchi, T. G. Hoang, and B. Ai, "Thermoelectronic breakdown with pressure and space charge effects in polyethylene," *J. Appl. Phys.*, vol. 81, no. 5, pp. 2363–2369, 1997.

[21] J. Artbauer, "Electric strength of polymers," *J. Phys. D, Appl. Phys.*, vol. 29, no. 2, pp. 446, 1996.

[22] L. A. Dissado and J. C. Fothergill, *Electrical Degradation and Breakdown in Polymers*, The Institution of Engineering and Technology, London, 1992, pp. 620.

[23] G. Blaise, "Charge localization and transport in disordered dielectric materials," *J. Electrostatics*, vol. 50, no. 2, pp. 69–89, 2001.

[24] S. Li, G. Yin, G. Chen, J. Li, S. Bai, L. Zhong, Y. Zhang, and Q. Q. Lei, "Short-term breakdown and long-term failure in nanodielectrics: A review," *IEEE Trans. Dielectr. Electr. Insul.*, vol. 17, no. 5, pp. 1523–1535, 2010.

[25] T. Mizutani and M. Ieda, "Carrier transport in high-density polyethylene," *J. Phys. D, Appl. Phys.*, vol. 12, no. 2, pp. 291, 2001.

[26] J. R. Dennison and J. Brunson, "Temperature and electric field dependence of conduction in low-density polyethylene," *IEEE Trans. Plasma Sci.*, vol. 36, no. 5, pp. 2246–2252, 2008.

[27] T. C. Zhou, G. Chen, R. J. Liao, and Z. Xu, "Charge trapping and detrapping in polymeric materials," *J. Appl. Phys.*, vol. 106, no. 12, pp. 123707, 2009.

[28] T. Zhou, G. Chen, R. Liao, and Z. Xu, "Charge trapping and detrapping in polymeric materials: Trapping parameters," *J. Appl. Phys.*, vol. 110, no. 4, pp. 043724, 2011.

[29] M. Meunier and N. Quirke, "Molecular modeling of electron trapping in polymer insulators," *J. Chem. Phys.*, vol. 113, no. 1, pp. 369–376, 2000.

[30] M. Meunier, N. Quirke, and A. Aslanides, "Molecular modeling of electron traps in polymer insulators: Chemical defects and impurities," *J. Chem. Phys.*, vol. 115, no. 6, pp. 2876–2881, 2001.

[31] Q. Lei, F. Tian, C. Yang, L. He, and Y. Wang, "Modified isothermal discharge current theory and its application in the determination of trap level distribution in polyimide films," *J. Electrostatics*, vol. 68, no. 3, pp. 243–248, 2010.

[32] P. Llovera and P. Molinie, "New methodology for surface potential decay measurements: Application to study charge injection dynamics on polypropylene films," *IEEE Trans. Dielectr. Electr. Insul.*, vol. 11, no. 6, pp. 1049–1056, 2016.

[33] P. K. Watson, "The transport and trapping of electrons in polymers," *IEEE Trans. Dielectr. Electr. Insul.*, vol. 2, no. 5, pp. 915–924, 2002.

[34] G. J. Zhang, K. Yang, M. Dong, W. B. Zhao, and Y. Zhang, "Surface electroluminescence phenomena correlated with trapping parameters of insulating polymers," *Appl. Surf. Sci.*, vol. 254, no. 5, pp. 1450–1455, 2007.

[35] W. B. Zhao, G. J. Zhang, Y. Yang, and Z. Yan, "Correlation between trapping parameters and surface insulation strength of solid dielectric under pulse voltage in vacuum," *IEEE Trans. Dielectr. Electr. Insul.*, vol. 14, no. 1, pp. 170–178, 2007.

[36] F. Tian, W. Bu, L. Shi, C. Yang, Y. Wang, and Q. Lei, "Theory of modified thermally stimulated current and direct determination of trap level distribution," *J. Electrostatics*, vol. 69, no. 1, pp. 7–10, 2011.

[37] K. C. Kao, *Dielectric Phenomena in Solids*. Elsevier: San Diego, CA, pp. 41–323, 2004.

[38] G. Teyssedre and C. Laurent, "Charge transport modeling in insulating polymers: From molecular to macroscopic scale," *IEEE Trans. Dielectr. Electr. Insul.*, vol. 12, no. 5, pp. 857–875, 2005.

[39] T. J. Lewis, "Interfaces are the dominant feature of dielectrics at the nanometric level," *IEEE Trans. Dielectr. Electr. Insul.*, vol. 11, no. 5, pp. 739–753, 2004.

[40] T. J. Lewis, "Interfaces: Nanometric dielectrics," *J. Phys. D, Appl. Phys.*, vol. 38, no. 2, pp. 202–212, 2005.

[41] T. Tanaka, M. Kozako, N. Fuse, and Y. Ohki, "Proposal of a multi-core model for polymer nanocomposite dielectrics," *IEEE Trans. Dielectr. Electr. Insul.*, vol. 12, no. 4, pp. 669–681, 2005.

[42] J. K. Nelson, "Dielectric Polymer Nanocomposites," Springer: New York, pp. 1–285, 2010.

[43] T. J. Lewis, "Charge transport in polyethylene nano dielectrics," *IEEE Trans. Dielectr. Electr. Insul.*, vol. 21, no. 2, pp. 497–502, 2014.

[44] P. O. Henk, "Increasing the electrical discharge endurance of acid anhydride cured DGEBA epoxy resin by dispersion of nanoparticle silica," *High Performance Polym.*, vol. 11, no. 11, pp. 281–296, 1999.

[45] S. L. Roy, P. Segur, G. Teyssedre, and C. Laurent, "Description of bipolar charge transport in polyethylene using a fluid model with a constant mobility: Model prediction," *J. Phys. D, Appl. Phys.*, vol. 37, no. 2, pp. 298–305, 2004.

[46] C. Laurent, G. Teyssedre, S. L. Roy, and F. Baudoin, "Charge dynamics and its energetic features in polymeric materials," *IEEE Trans. Dielectr. Electr. Insul.*, vol. 20, no. 2, pp. 357–381, 2013.

[47] F. Boufayed, G. Teyssedre, C. Laurent, S. Le Roy, L. A. Dissado, P. Segurm, and G. C. Montanari, "Models of bipolar charge transport in polyethylene," *J. Appl. Phys.*, vol. 100, no. 10, pp. 826–356, 2006.

[48] G. Chen, "A new model for surface potential decay of corona-charged polymers," *J. Phys. D, Appl. Phys.*, vol. 43, no. 5, pp. 55405–55411, 2010.

[49] D. Min, W. Wang, and S. Li, "Numerical analysis of space charge accumulation and conduction properties in LDPE nanodielectrics," *IEEE Trans. Dielectr. Electr. Insul.*, vol. 22, no. 3, pp. 1483–1491, 2015.